Supporting information

Robust, UV-resistant and transparent vitrimers from bio-based mercaptan via maleimide-thiol "click" chemistry for carbon fiber reinforced polymer composites

Yue Wang, Jialiang Zhong, Yanning Zeng*
College of Material Science and Engineering, Guilin University of Technology, Guilin 541004, P. R. China
* Corresponding author, E-mail:ynzeng@glut.edu.cn

Scheme S1 Synthesis of E-4SH

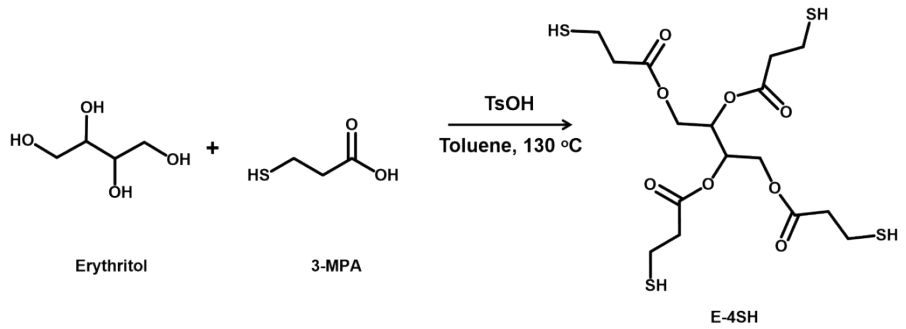

Scheme S2 Synthesis of G-3SH

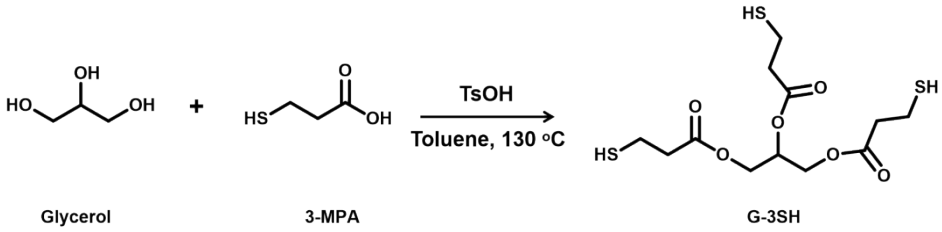

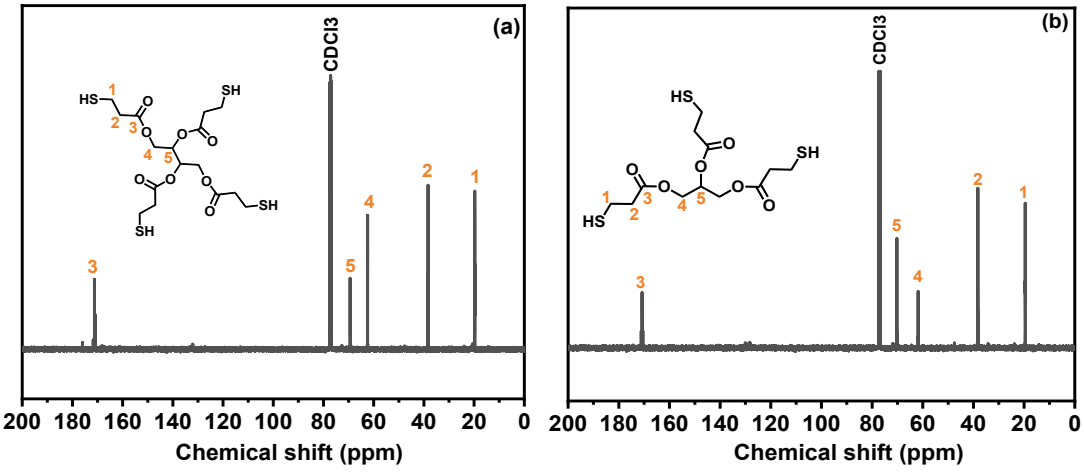

Fig. S1 ^{13}C NMR spectrum of (a) E-4SH and (b) G-3SH

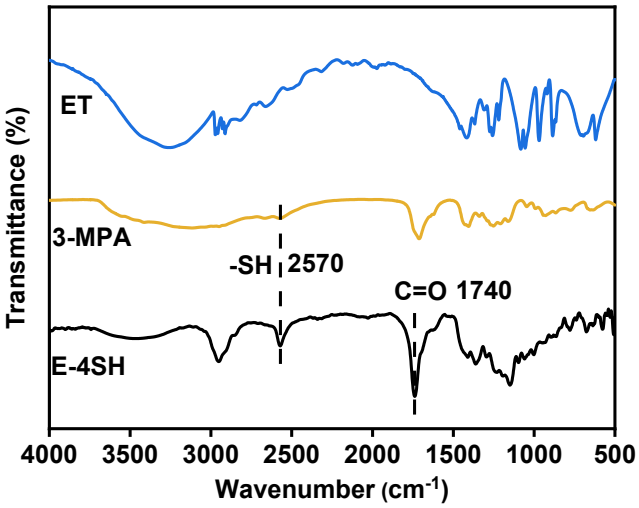

Fig. S2 FTIR spectra of ET, 3-MPA, E-4SH

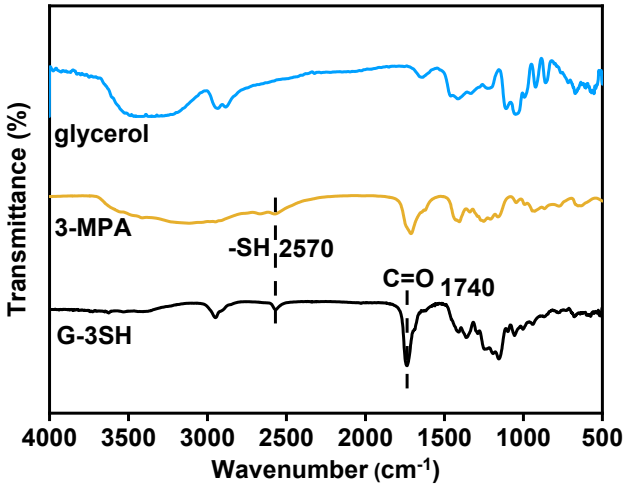

Fig. S3 FTIR spectra of glycerol, 3-MPA, G-3SH

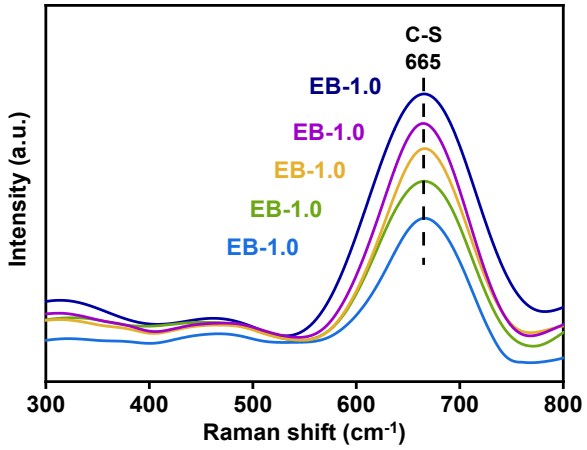

Fig. S4 Raman spectra of EB-x series

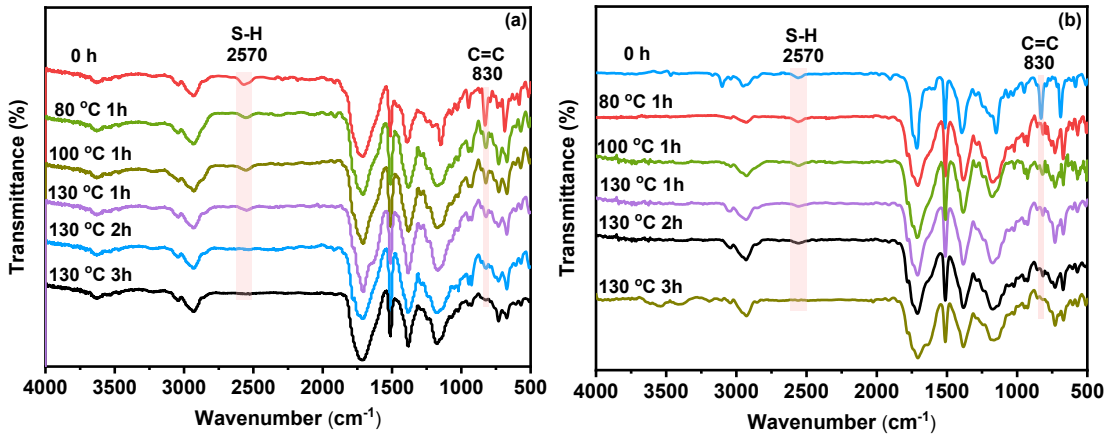

Fig. S5 Thermal curing process of (a) EB-1.0 and (b) GB-1.0 monitored by FTIR spectroscopy.

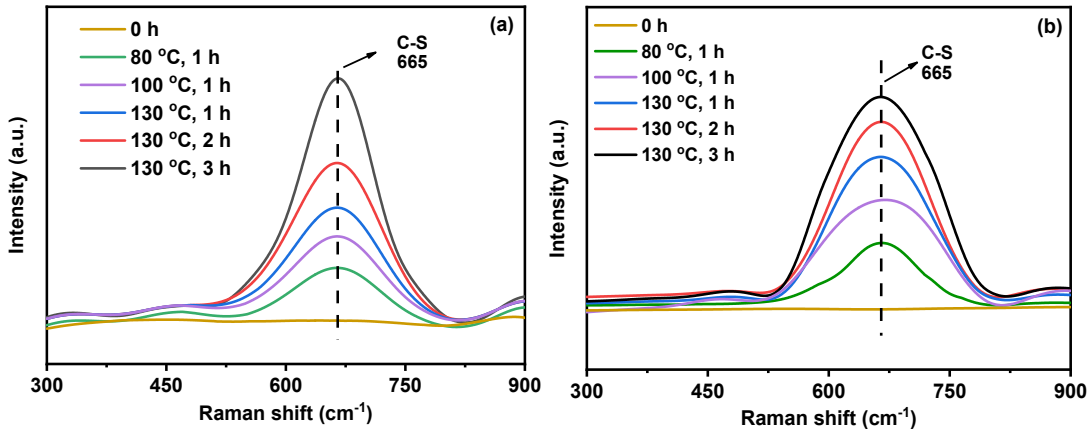

Fig. S6 Thermal curing process of (a) EB-1.0 and (b) GB-1.0 monitored by Roman spectroscopy

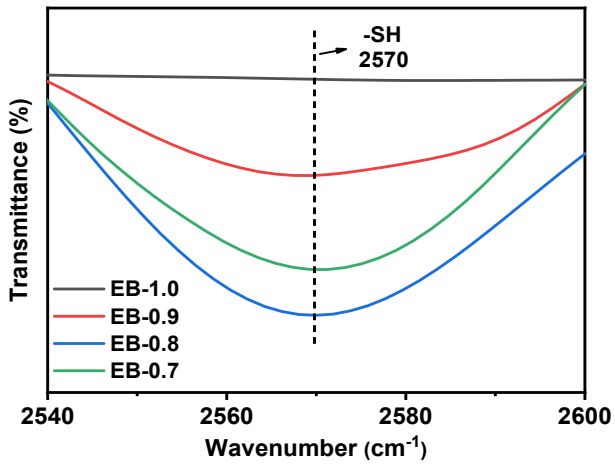

Fig. S7 Normalized FTIR spectra of EB-x in the range from 2500 to 2600 cm^{-1}

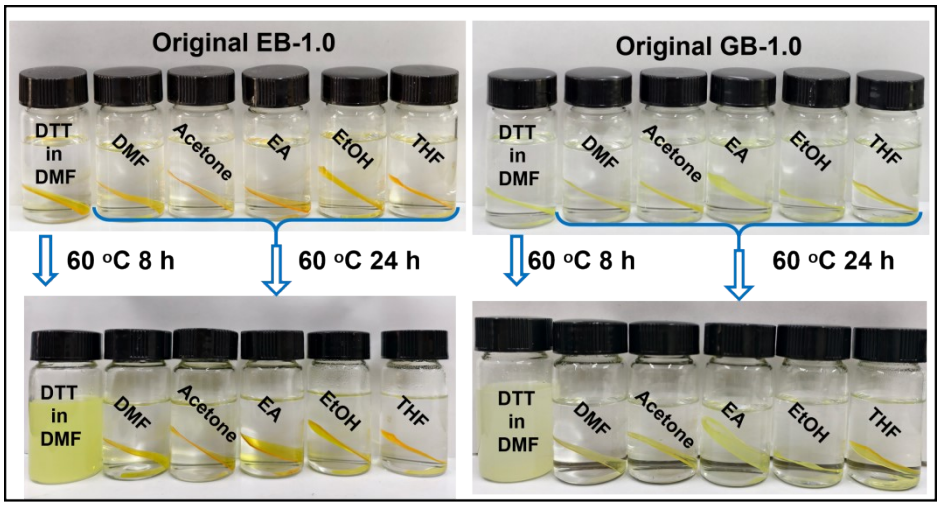

Fig. S8 Solvent resistance of EB-1.0 and GB-1.0 in different solvents

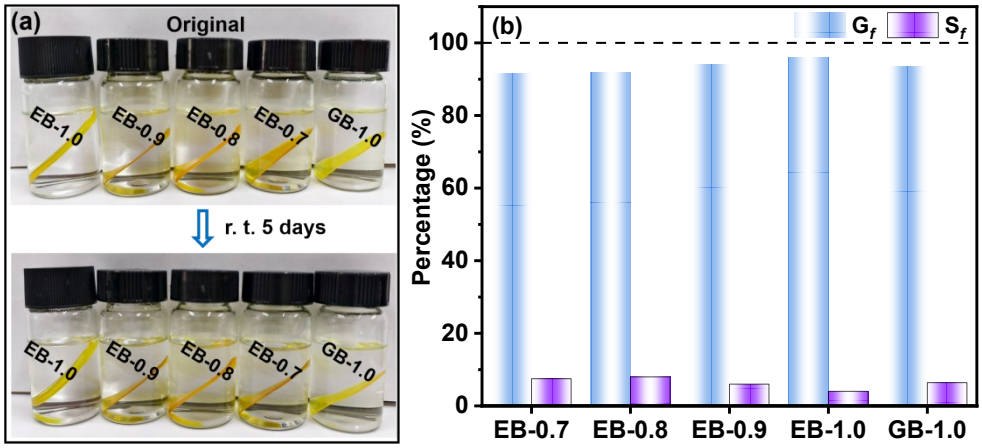

Fig. S9 (a) Swelling tests and (b) Gel fractions (G_f) and soluble fractions (S_f) of EB-x and GB-1.0 after immersion in DMF for 5 days at room temperature

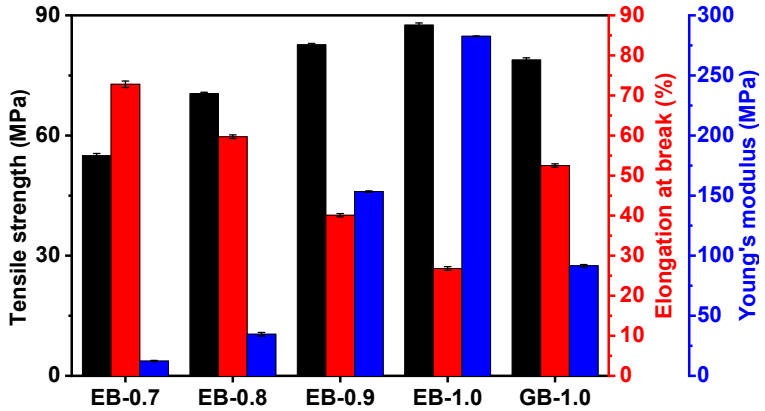

Fig. S10 Mechanical properties of EB-x and GB-1.0

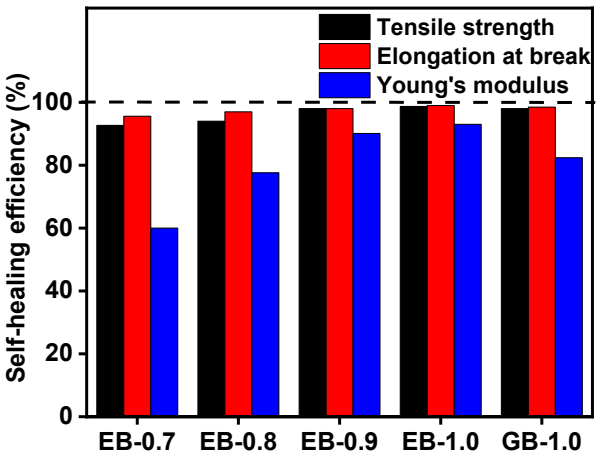

Fig. S11 Self-healing efficiency of EB-x and GB-1.0

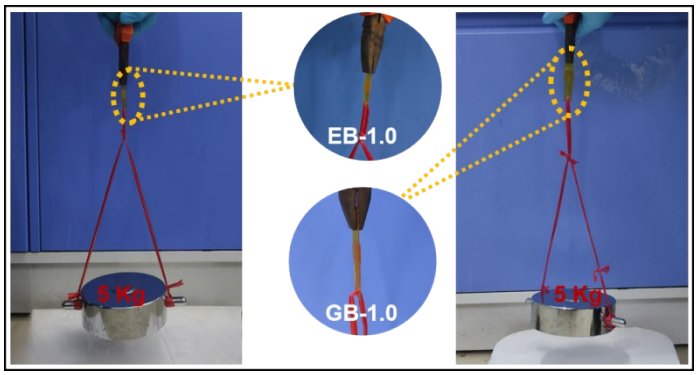

Fig. S12 Digital images of a welded EB-1.0 and GB-1.0 under a loading

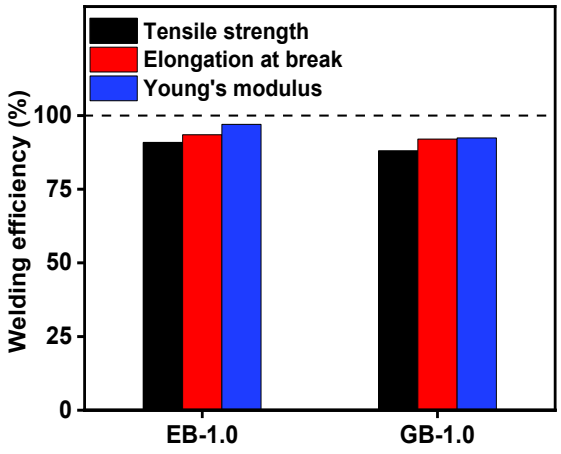

Fig. S13 Welding efficiency of EB-1.0 and GB-1.0

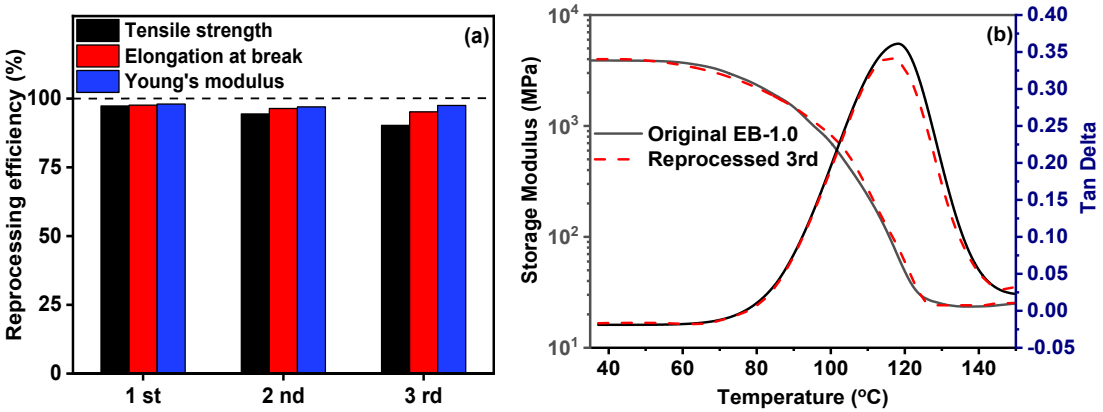

Fig. S14 (a) Reprocessing efficiency and (b) DMA curve of the reprocessed of EB-1.0

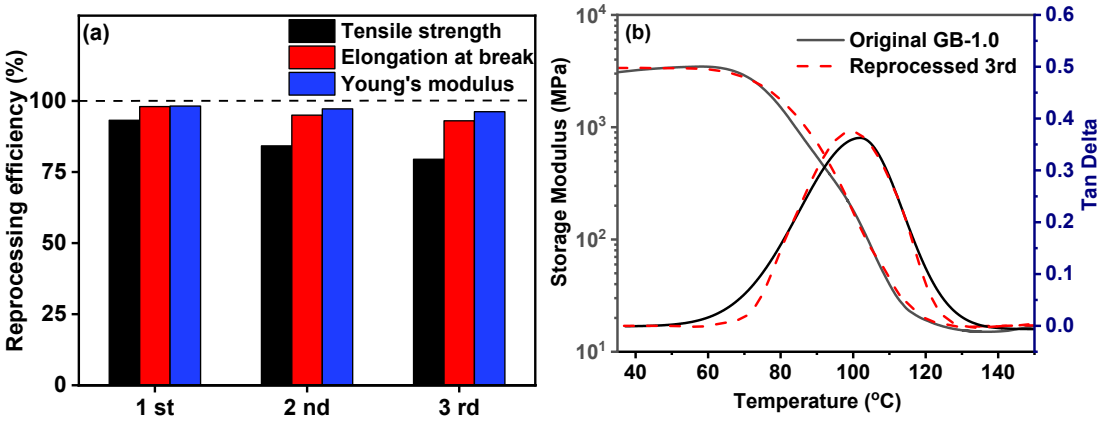

Fig. S15 (a) Reprocessing efficiency and (b) DMA curve of the reprocessed of GB-1.0

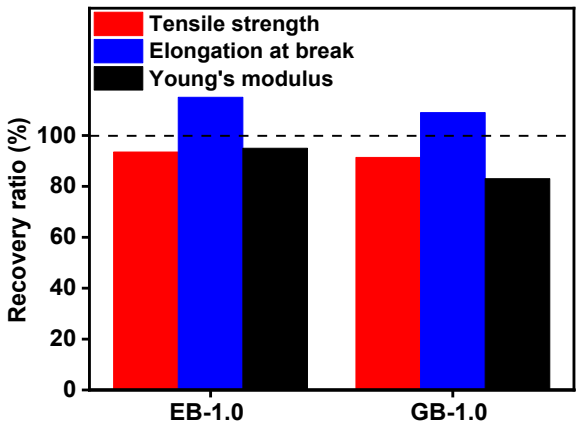

Fig. S16 Recovery ratio of the recycled EB-1.0 and GB-1.0

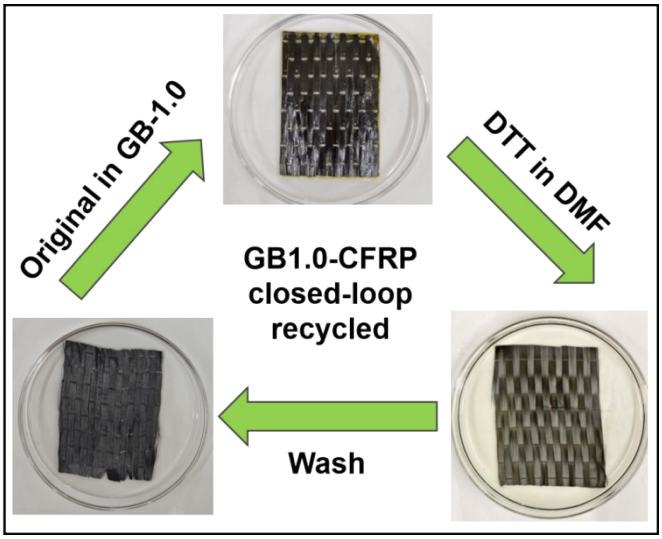

Fig. S17 Digital images of recycling of GB-1.0-based CFRP composite